2021 43rd Annual International Conference of the
IEEE Engineering in Medicine & Biology Society (EMBC)
Oct 31 - Nov 4, 2021. Virtual Conference

A computational study of the relation between the power density in the tumor and the maximum temperature in the scalp during Tumor Treating Fields (TTFields) therapy

Nichal Gentilal[1], Ariel Naveh[2], Tal Marciano[2], Zeev Bomzon[2], Yevgeniy Telepinsky[2], Yoram Wasserman[2] and Pedro Cavaleiro Miranda[1]

***Abstract*— In this work we investigated the relation between the power density in the tumor and the maximum temperature reached in the scalp during TTFields treatment for glioblastoma. We used a realistic head model to perform the simulations in COMSOL Multiphysics and we solved Pennes' equation to obtain the temperature distribution. Our results indicate that there might be a linear relation between these two quantities and that TTFields are safe from a thermal point of view.**

***Clinical Relevance*— This work shows that it might be possible to predict treatment effectiveness based on the temperature of the scalp.**

I. Introduction

Tumor Treating Fields (TTFields) is an FDA-approved anti-mitotic cancer treatment technique used for glioblastoma multiforme (GBM) and for pleural mesothelioma. It consists in applying an electric field (EF) with a frequency between 100 and 500 kHz in two perpendicular directions alternately for long periods of time. The biophysical mechanisms of action of this technique are thought to be twofold and consist mainly in the disruption of the mitotic spindle and movement of intracellular components to affect cell division. Analyses of clinical trials data showed a strong dependence of the effectiveness of this technique on the treatment time [1], which should be at least 18 hours per day for recurrent cases, and field intensity, which should be at least 1 V/cm at the tumor bed [2]. For GBM treatment, two pairs of transducer arrays are strategically placed on the shaved scalp based on the output of a software named NovoTAL™. This FDA-approved system creates individualized treatment maps that optimize the EF delivery based on the tumor location, head size and geometry. To avoid thermal harm to head tissues, the device used to apply TTFields in patients, Optune®, monitors the temperature on the surface of the scalp and keeps it below 39.5ºC. In this work we study the relation between the maximum temperature in the scalp and the EF in the tumor using a realistic head model.

II. Methods

We used the same realistic head model as in our previous studies on heat transfer during TTFields [3,4]. This model is segmented into scalp, skull, cerebrospinal fluid (CSF) and brain (grey matter plus white matter). A spherical virtual lesion was added in the right hemisphere, near the lateral ventricle, to mimic a GBM tumor. The latter consisted in a necrotic core surrounded by an enhancing region. The position of the arrays (fig. 1) was obtained through the NovoTAL system and the final meshes were built in Materialise 3-matic. In this software, a thin layer was added between each transducer and the scalp to mimic the gel, which allows current to flow into the head. The simulations were performed in COMSOL Multiphysics v.5.2 using the AC/DC (electric currents interface) and the heat transfer (heat transfer in solids interface) modules. The first one was used to calculate the EF distribution in the head at 200 kHz for the anterior-posterior (AP) and left-right (LR) configurations using Laplace's equation. The second one was used to predict the temperature distribution in each tissue through Pennes' equation:

$$\rho\, c\, \frac{\partial T}{\partial t} = \nabla \cdot (k \nabla T) + \omega \rho_b c_b (T_b - T) + Q_m + \sigma \|\boldsymbol{E}\|^2 \quad (1)$$

where ρ represents the density (kg m^{-3}), c the specific heat (J $kg^{-1}ºC^{-1}$), T the temperature (ºC), k the thermal conductivity (W $m^{-1}ºC^{-1}$), ω the blood perfusion (s^{-1}), Q_m the metabolic heat (W m^{-3}), which was assumed to be constant, σ the electric conductivity (S m^{-1}) and **E** the electric field vector (V m^{-1}). The subscript b stands for blood. Energy exchange with the environment through convection and radiation was also considered. The value of

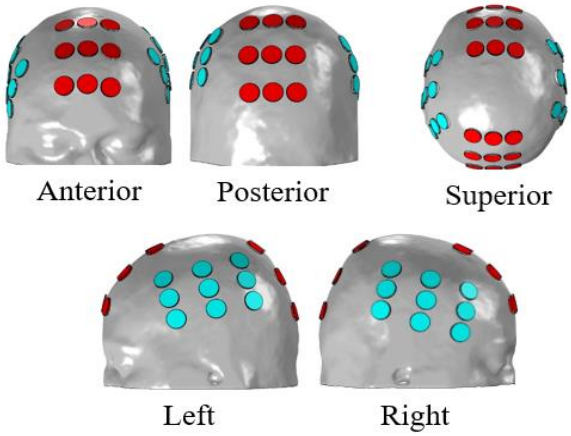

Fig. 1: Different views of the head model built using a realistic array layout. The anterior-posterior (AP) configuration is colored as red whereas the left-right (LR) configuration is in light blue.

[1]N. Gentilal (ngentilal@fc.ul.pt) and P.C. Miranda are with the Instituto de Biofísica e Engenharia Biomédica (IBEB), Faculdade de Ciências, Universidade de Lisboa, Campo Grande, 1749-016, Lisboa, Portugal.

[2]A. Naveh, T. Marciano, Z. Bomzon, Y. Telepinsky and Y. Wasserman are with Novocure, Topaz Building, 4th floor, MATAM center, PO Box 15022, Haifa, Israel.

each electric parameter was taken from [2] whereas the thermal properties were considered to be the standard values reported in [4]. All tissues and materials were assumed to be homogenous and isotropic.

To allow for reasonable computational times, we simplified the current injection algorithm by assuming that current was injected into the anterior-posterior (AP) and left-right (LR) configurations alternately with a switching time of one second. We investigated how much current could be injected into each configuration by predicting the maximum temperature that the scalp would reach, as described in the results section. Following the same approach as in [2], we then quantified the EF and the power density (PD) in a volume of interest (VOI) containing the enhancing tumor plus a 3-mm proximal boundary surrounding it. The values were taken for each voxel (1 mm x 1 mm x 1 mm) within this VOI. In this head model and for this specific tumor location this volume was occupied by white matter (62%), enhancing tumor (35%), grey matter (2%) and CSF from the lateral ventricles (1%). The power density is defined as:

$$Power\ density\ (W\ m^{-3}) = \sigma \|\boldsymbol{E}\|^2 \qquad (2)$$

Comparing equations (1) and (2) it can be seen that the mathematical expression of the PD is the same as of the Joule effect. This shows that there has to be a trade-off between the PD, which should be maximized, and the temperature increases in head tissues, which should be within a safety range, to optimize TTFields therapy.

III. Results

As described in detail in [3] the regions underneath the transducers are the ones where tissues reach the maximum temperature. Furthermore, temperature maxima in each tissue are reached at the surface and quickly drop with depth. Thus, the surface of the scalp underneath the transducers, which is where the Optune system monitors the temperature, is the region where the temperature will increase most during treatment.

Fig. 2 shows the maximum temperature in these regions underneath the AP and LR configurations as a function of time for different values of injected current. Each simulation took around 34 h to compute in a workstation with a 2 x 8-core CPU's (Intel i7-9800X CPU @ 3.80 GHz) and 64 GB RAM. Given that it would not be practical to wait for the scalp to reach a steady state temperature in all these simulations, a different approach had to be used to predict the maximum temperature that it would reach.

Considering the behavior of the temperature variation, an expression such as eq. (3) can be fitted to each curve in fig. 2:

$$T = C_1(1 - exp(-C_2 t)) + C_3 \qquad (3)$$

In this context, C_1 (in ºC) represents the maximum contribution of the injected current in increasing the temperature, C_2 (in s^{-1}) is related to how quick is the heat transferred and C_3 (in ºC) is the initial temperature of the scalp. The maximum temperature (T^{max}) can then be predicted by taking the limit of $t \to \infty$ which results in $C_1 + C_3$. These and

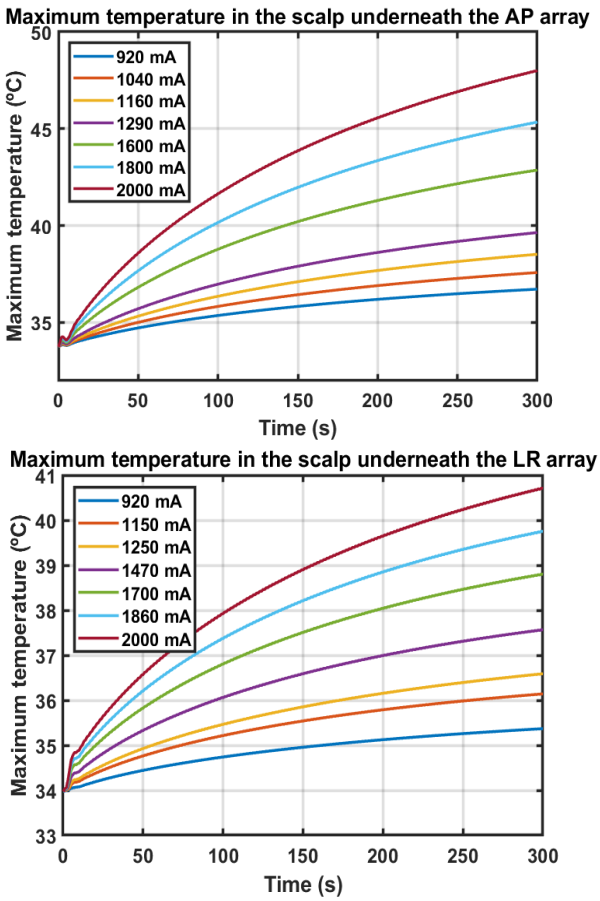

Fig. 2: Maximum temperature variation on the scalp surface for 5-minutes simulations underneath the AP and LR (upper and lower plots, respectively) arrays. Note the different values of injected current (peak-to-peak) into each configuration and the different temperatures scales.

all the other fits performed throughout this work were done using MATLAB's curve fitting toolbox. The minimum adjusted R^2 (A-R^2) obtained for the data shown in fig. 2 was 0.998.

For each one of these curves, the maximum temperature in the scalp was predicted and it is presented in fig. 3 alongside with the average PD in the VOI as a function of the injected current. In the latter figure, it is possible to see that the power density varies quadratically with the injected current. This is expected given how the first is mathematically defined and the linear dependence between the injected current and the induced EF. Curve fitting of these data led to the following equations:

$$PD_{AP} = (2.97 \times 10^{-7}) I_{AP}^2 \qquad (4)$$

$$PD_{LR} = (9.62 \times 10^{-7}) I_{LR}^2 \qquad (5)$$

The A-R^2 was 1 for both these fits. Looking at fig. 3 it is noticeable that the temperature variation follows the same behavior as the PD. Thus, we also assumed a quadratic dependence between the temperature and the injected current to which we added a constant to account for the initial temperature of the scalp when no EFs are applied:

$$T_{AP}^{max} = (4.13 \times 10^{-6}) I_{AP}^2 + 33.83 \qquad (6)$$

$$T_{LR}^{max} = (1.87 \times 10^{-6}) I_{LR}^2 + 34.06 \qquad (7)$$

The A-R^2 was 0.9999 for the first equation and 0.9993 for the second. We fitted other equations to these data (exponentials and first- and second-degree polynomials), but the goodness of the fit was lower.

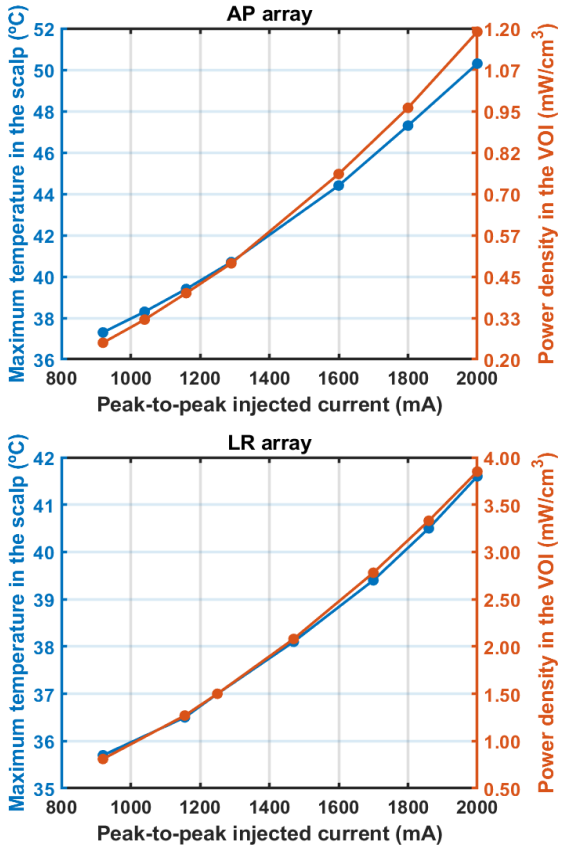

Fig. 3: Variation of the maximum temperature predicted in the scalp (blue lines) and average power density in the volume of interest (orange lines) as a function of the current injected in the AP and LR (upper and lower plots, respectively) configurations.

In equations (4) to (7) the PD values are in mW cm^{-3}, T^{max} in ºC and I is the injected current (peak-to-peak) in mA.This means that there may be an approximately linear relationship between T^{max} and PD. Performing a linear curve fit to these data the following equations were obtained:

$$T_{AP}^{max} = 13.88\, PD_{AP} + 33.86 \quad (8)$$

$$T_{LR}^{max} = 1.94\, PD_{LR} + 34.08 \quad (9)$$

The A-R^2 was 0.9998 for the first and 0.9994 for the second.

Additionally, and following the same approach as for the scalp, we predicted the maximum temperature that would be reached in the skull, CSF, brain and enhancing tumor for the values of current that led to a maximum temperature of 39.5ºC in the scalp (1160 mA in the AP configuration and 1700 mA in the LR). The temperature variation for each one of these tissues can be seen in fig. 4. Temperature maxima occurred at the surface of each tissue and the maximum value predicted was 39.4ºC in the skull, 38.0ºC in the CSF (located in the lateral ventricles), 37.8ºC in the brain and 38.3 ºC in the tumor.

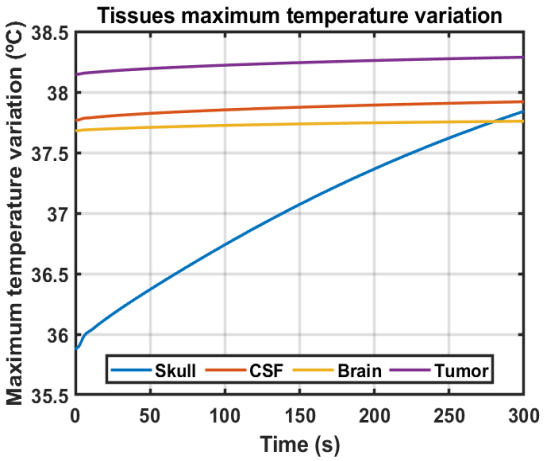

Fig. 4: Variation of the maximum surface temperature in the skull, CSF (from the lateral ventricles), brain and enhancing tumor when 1160 mA were injected into the AP configuration and 1700 mA into the LR.

IV. Discussion

The variation of the maximum temperature of the scalp follows a similar behavior independently of the injected current and of the array layout, as shown in fig. 2. In this model and for this tumor location, the maximum current that can be injected to reach the maximum temperature of 39.5ºC in the scalp is 1160 mA in the AP configuration and 1700 mA in the LR, peak-to-peak values (fig. 3). Less current can be injected into the first because the resistance of the head is higher in the AP direction. For the injected currents mentioned above the average PD in the volume of interest was also lower in the AP configuration, 0.40 mW/cm^3, than in the LR's, 2.78 mW/cm^3. A recent study [2] used data from TTFields clinical trials to quantify the PD value that best divides GBM patients into two groups with the greatest statistical difference in the overall survival (OS) and yielded 1.15 mW/cm^3. Patients whose average PD was higher than this threshold had an overall survival of 24.9 months, whereas the group of patients with a power density below this value had an OS of 21.5 months.

Our results indicate that the EF produced by the LR arrays contributes significantly more to treatment than the EF induced by the AP arrays, which is explained by the location of the virtual lesion in this model and by the simplified representation of the GBM tumor. This lesion was placed midway between the AP arrays and very close to the lateral ventricles, where the electric field magnitude produced by this configuration reaches the lowest values in the brain. Additionally, the fact that the tumor is not based on real MR data might affect the EF distribution due to its size and lack of representation of some tissues such as the enhancing nontumor tissue, the ischemic region and hematoma, which were represented in the study that derived the thresholds mentioned above [2].

In the aforementioned work, an additional metric was defined to account for the fact that TTFields are delivered in two directions. The local minimum power density (LMiPD) corresponds to the lowest of the two PDs delivered to each voxel within the volume of interest. As discussed above, the electric field produced by the AP configuration is much lower than that produced by the LR configuration and thus the

average LMiPD is significantly affected by the values of the first, yielding 0.40 mW/cm^3. Clinically, dose density might be reported instead of the power density. The dose is defined as the PD multiplied by the fraction of the daily time that the patient is subjected to the EFs, which has been shown to be an important factor in the OS.

The results we obtained also showed that the maximum temperature in the scalp might vary quadratically with the injected current, which could be surprising at first if one looks at Pennes' equation (eq. 1). Through this equation, it is possible to see that when the temperature increases due to the Joule effect, more energy should also be transferred through conduction (first term on the right side) and through blood perfusion (second term on the right side). The rate at which heat is dissipated depends on the thermal conductivity (k), blood perfusion rate (ω), density (ρ) and specific heat (c) of the scalp, as well as on the temperature difference between the hottest and cooler regions. However, the Joule effect term (fourth term on the right side) appears when the EFs start to be applied and it does not depend on a temperature gradient between regions. This explains why the temperature tends asymptotically to a steady-state value, as described by eq. (3). The quick rise is due to the application of the fields and the more current is injected the highest the maximum temperature. At some stage, the temperature gradient becomes high and more energy starts to be transferred through conduction and perfusion, which will result in a steady state temperature in the scalp. It is noteworthy that in a previous work [4] we showed that in the hottest regions the Joule effect explained practically 100% of the temperature increases in the scalp, whereas metabolic heat (third term on the right side of Pennes' equation) had a negligible impact. On the other hand, most of the cooling in this tissue was explained by conduction to the cooler regions of the scalp, to the gel and to the deepest tissues.

This explains why the maximum temperature that the scalp reaches is highly affected by the Joule effect and consequently why there is a strong linear relationship between the power density and temperature maxima. This dependence was different for each configuration and the coefficients of the fitted curve will most likely be very specific to each array layout and patient. Nonetheless, if the position of the layout does not change significantly throughout treatment, it may be possible to predict the effectiveness of the therapy based on the temperature of the scalp.

The skull, CSF, brain and tumor follow the same temperature variation behavior as the scalp (fig. 4). As expected, the deeper the tissue the higher the initial temperature and closer to blood's temperature. Among these four, the skull is the one whose temperature varied the most. By fitting eq. (3) to the data we predict a maximum temperature in the skull at the hottest region of 39.4ºC (+3.5ºC) when the scalp's temperature reaches 39.5ºC. The temperature of the remaining three tissues varied much less relative to their initial value: +0.2ºC in the ventricular CSF, +0.1ºC in the brain and +0.2ºC in the enhancing tumor.

In a previous work [3] we predicted the thermal impact of TTFields assuming that Optune monitors the temperature of the transducers and that the optimal working point was 41ºC instead of 39.5ºC in the scalp. These assumptions led us to predict some physiological changes in the brain such as variation in the concentration of some neurotransmitters and an increase of the blood-brain barrier permeability according to the temperature values we had. In this work, we improved the modelling of the conditions in which therapy occurs and these previous conclusions do not hold anymore. Based on the literature and for the temperature range obtained, what is expected when the temperature increases in the brain is an increase of the blood flow and metabolic rate [5]. These are biological mechanisms that help to dissipate heat more efficiently. Up until now, the only side-effect seen in TTFields patients is skin dermatitis underneath the regions where the transducers are placed due to the use of the hydrogel [6]. Adverse effects due to the temperature increases were not reported and are not likely to occur according to the results we presented here.

V. Conclusion

The results obtained in this work showed that there is an approximately linear relation between the maximum temperature reached in the scalp and the average power density at the tumor bed during TTFields treatment for glioblastoma. Even though it is very likely that the fit coefficients are array and patient dependent, knowing how effective the technique might be based on the temperature of the scalp can be very useful.

Our results indicate that for the temperature range at which the Optune device operates, TTFields are safe from a thermal point of view. In future work, it might be necessary to improve our model by considering a more realistic representation of the tumor.

Conflict of Interests

IBEB is funded by Fundação para a Ciência e Tecnologia (FCT), Portugal, under grant nº UIDB/00645/2020. P. C. Miranda has a research agreement funded by Novocure. N. Gentilal holds a PhD grant funded by this agreement. A. Naveh, T. Marciano, Z. Bomzon, Y. Telepinsky and Y. Wasserman are employed by, and hold stock in, Novocure.

References

[1] A. Kanner, E. T. Wong, J. L. Villano, Z. Ram and EF-11 investigators, "Post hoc analyses of intention-to-treat population in phase III comparison of NovoTTF-100A system versus best physician's choice chemotherapy," *Semin Oncol* vol. 41, Suppl. 6, pp. S25-S34, 2014

[2] M. T. Ballo, N. Urman, G. Lavy-Shahaf, J. Grewal, Z. Bomzon and S. Toms, "Correlation of Tumor Treating Fields dosimetry to survival outcomes in newly diagnosed glioblastoma: a large-scale numerical simulation-based analysis of data from the phase 3 EF-14 randomized trial," *Int J Radiat Oncol Biol Phys* vol. 104, no. 5, pp. 1106-13, 2019

[3] N. Gentilal, R. Salvador and P. C. Miranda, "Temperature control in TTFields therapy of GBM: impact on the duty cycle and tissue temperature,", *Phys Med Biol*, vol. 64, no. 22, pp. 225008, 2019.

[4] N. Gentilal and P. C. Miranda, "Heat transfer during TTFields treatment: Influence of the uncertainty of the electric and thermal parameters on the predicted temperature distribution", *Computer Methods and Programs in Biomedicine*, vol. 196, pp. 105706, 2020.

[5] H. L.Rosomoff and D. A. Holaday, "Cerebral blood flow and cerebral oxygen consumption during hypothermia", *Am J Physiol*, vol. 179, no. 1, pp. 85-8, 1954.

[6] R. Stupp, S. Tailibert, A. Kanner, Z. Ram, et al "Effect of Tumor Treating Fields plus maintenance temozolomide vs maintenance temozolomide alone on survival in patients with glioblastoma: a randomized clinical trial", *JAMA*, vol. 318, no. 12, pp. 2306-16, 2017.